frontiers | Frontiers in Immunology

TYPE Original Research
PUBLISHED 25 August 2025
DOI 10.3389/fimmu.2025.1628194

OPEN ACCESS

EDITED BY
Amy L. Kenter,
University of Illinois Chicago, United States

REVIEWED BY
Michael William Washabaugh,
The MITRE Corporation, United States
Marcus O. Muench,
Vitalant Research Institute, United States

*CORRESPONDENCE
Melanie C. Dispenza
mdispen1@jhmi.edu

RECEIVED 13 May 2025
ACCEPTED 15 July 2025
PUBLISHED 25 August 2025

CITATION
Lin EV, Krier-Burris RA, Sokol KA, Arce B, Vilela NM, Hamilton RG, Bochner BS and Dispenza MC (2025) Engrafted NSG-SGM3 humanized mice spontaneously produce human immunoglobulins including IgE. *Front. Immunol.* 16:1628194. doi: 10.3389/fimmu.2025.1628194

Engrafted NSG-SGM3 humanized mice spontaneously produce human immunoglobulins including IgE

Erica V. Lin[1], Rebecca A. Krier-Burris[2], Kristina A. Sokol[1], Betania Arce[1], Natalia M. Vilela[1], Robert G. Hamilton[1], Bruce S. Bochner[2] and Melanie C. Dispenza[1*]

[1]Division of Allergy and Clinical Immunology, Department of Medicine, Johns Hopkins University School of Medicine, Baltimore, MD, United States, [2]Division of Allergy and Immunology, Department of Medicine, Northwestern University Feinberg School of Medicine, Chicago, IL, United States

NSG-SGM3 humanized mouse models are well-suited for studying human immune physiology but are technically challenging and expensive. We previously characterized a simplified NSG-SGM3 mouse, engrafted with human donor CD34$^+$ hematopoietic stem cells without receiving prior bone marrow ablation or human secondary lymphoid tissue implantation, that still retains human mast cell- and basophil-dependent passive anaphylaxis responses. Its capacities for human antibody production and human B cell maturation, however, remain unknown. Here, we show that NSG-SGM3 mice engrafted without prior marrow ablation spontaneously produce all human antibodies, including IgE, without deliberate sensitization. These human IgE antibodies are polyclonal with unexpected specificities to diverse allergens, such as millet, egg, and wasp venom, that are otherwise absent from the mouse diet or housing environments. Furthermore, human CD138$^+$ CD27$^+$ plasma cell and CD20$^+$ CD27$^+$ memory B cell populations can be expanded from naïve engrafted NSG-SGM3 splenocytes in response to human CD40L and IL-4 cytokine stimulation *ex vivo*. Engrafted NSG-SGM3 mice, but not non-engrafted controls, also exhibit dose-dependent passive systemic anaphylaxis responses when challenged with goat anti-human IgE. In contrast, no anaphylaxis responses were observed in humanized NSG-SGM3 mice challenged with select food allergens. Together, our results demonstrate that engrafted NSG-SGM3 mice without prior ablation spontaneously produce abundant functional human antibodies, including polyclonal IgE that can facilitate anaphylaxis. These mice also unexpectedly possess the upstream capacity to support human B cell maturation into antibody-producing plasma cells and memory B cells. Our simpler humanized NSG-SGM3 model therefore reveals novel insights into dynamics of human B cell maturation, homing, and differentiation that facilitate the generation of a basal, functional, polyclonal IgE repertoire without deliberate sensitization.

KEYWORDS

anaphylaxis, B cell, humanized mice, IgE, NSG-SGM3

1 Introduction

Humanized mouse models are powerful tools for studying aspects of human immune physiology not fully reconstituted by the native murine immune system (1–3), such as allergy and anaphylaxis. A common humanized mouse model is the nonobese diabetic severe combined immunodeficiency common gamma chain-deficient (NOD *scid* gamma; NSG) mouse. NSG mice are immunodeficient and thus suitable for humanization due to mutations in IL-2R common gamma chain to deplete natural killer cells and *Prkdc* (*scid*) to deplete B and T cells (2–4). Traditional NSG models involve a three-pronged approach for humanization: (1) irradiation or chemical ablation of murine host bone marrow, (2) surgical implantation of human fetal liver and/or thymic tissue, and (3) engraftment with human $CD34^+$ hematopoietic stem cells (HSCs) (5–8). This older approach to creating "bone marrow, liver, thymus" (BLT) mice assumes that the original murine hematopoietic compartment may interfere with human HSC engraftment, and that endogenous murine lymphoid tissues are not sufficient milieus to support functional human HSC maturation without additional human lymphoid implants.

The next-generation NSG-SGM3 (NOD *scid*-IL2Rg^{null}-3/GM/SF) strain additionally expresses human transgenes for SCF, GM-CSF, and IL-3, cytokines which support the survival, proliferation, and maturation of human hematopoietic-derived granulocytes, including mast cells and basophils, even without implantation of human lymphoid tissue (4, 9–11). As a result, both BLT NSG-SGM3 mice as well as NSG-SGM3 mice engrafted after prior irradiation but lacking lymphoid explants can undergo passive systemic anaphylaxis (PSA) that is driven by human mast cells and basophils in response to allergen challenge (5, 12, 13). NSG-SGM3 mice are thus well-suited for modeling granulocyte- and IgE-dependent allergic responses and anaphylaxis in humans (9, 11, 12). Creating these mice, however, is very time-consuming and expensive. Furthermore, NSG-SGM3 mice engrafted after irradiation are prone to developing lymphomas and hemophagocytic lymphohistiocytosis (HLH)-like and/or macrophage activation syndrome (MAS)-like pancytopenia with older age (14–17).

We previously characterized a newer and simplified model of humanized NSG-SGM3 mice which are engrafted without prior bone marrow ablation or human lymphoid tissue implantation. In our model, 3–4-week-old NSG-SGM3 mice receiving one intravenous injection of human cord blood HSCs without preconditioning were similarly capable of supporting robust human HSC engraftment, including mature human mast cells and basophils, by 16 weeks post-injection, while their residual murine $CD45^+$ leukocytes dwindled over time (8). Notably, PSA responses for our simplified model were just as robust as for BLT mice (5, 8), suggesting that the physiology of human HSC maturation and downstream anaphylaxis remain intact despite present residual host murine immune cells. Furthermore, NSG-SGM3 mice without prior irradiation survive longer without HLH-like post-engraftment complications despite comparable HSC engraftment efficiency (14). These data put forth several advantages of our simplified model, especially in light of its intact granulocyte physiology.

It still remains unknown, however, whether NSG-SGM3 mice engrafted without prior marrow ablation can also support human antibody production and human B lymphocyte development. While NSG-SGM3 mice engrafted after irradiation and BLT NSG-SGM3 mice have been shown to make basal serum human IgM and IgG at older age (4, 18), these mice are again prone to severe immune dysregulation (15), with possibly lowly- or non-functional antibody. In addition, NSG-SGM3 mice engrafted without prior ablation or human tissue lymphoid implantation make peanut-specific IgE after oral gavage with peanut, which suggests some functional human plasma cell differentiation (11). It is therefore poorly understood whether human HSC-derived human B cells can produce functional human antibody in the setting of a non-ablated murine background in NSG-SGM3 mice, as well as why these human B cells can survive in host murine lymphoid milieus without human lymphoid tissue.

Here, we show for the first time that NSG-SGM3 humanized mice engrafted without prior ablation can produce spontaneous human antibodies of all isotypes without deliberate sensitization, including polyclonal and functional human IgE. Our work also characterizes the human antibody and cytokine landscapes and identifies putative Th2 cytokine-responsive B cell populations in our simplified NSG-SGM3 humanized mouse model, with an additional novel focus on functional profiling of human IgE.

2 Materials and methods

2.1 Mice

C57BL/6J wildtype ("WT"; "B6"; 000664) and NOD.Cg-*Prkdc*^{scid} *Il2rg*^{tm1Wjl} Tg(CMV-*IL3,CSF2,KITLG*)1Eav mice ("NSG-SGM3"; 013062) were purchased from Jackson Laboratory. All mice were female sex and littermates unless otherwise stated and maintained in barrier housing in specific-pathogen free animal facilities on the Johns Hopkins Bayview Medical Center campus.

NSG-SGM3 mice were engrafted as previously described at 3–4 weeks old with a single retroorbital injection of 5 x 10^5 human cord blood $CD34^+$ cells (Lonza Poietics) resuspended in sterile PBS (Sigma) (8). Successful engraftment of human cells was confirmed 12 weeks after injection using flow cytometry analysis of whole blood stained with appropriate fluorescent antibodies and processed on a BD Accuri C6 cytometer (BD Biosciences) as previously described (8). Serum samples were collected via retroorbital bleed after 16 weeks of engraftment and at least two weeks prior to splenocyte culture.

Abbreviations: B6, C57BL/6J; BLT, "bone marrow, liver, thymus"; HLH, hemophagocytic lymphohistiocytosis; HSC(s), hematopoietic stem cell(s); MAS, macrophage activation syndrome; MBC, memory B cell(s); NSG, NOD *scid* gamma; NSG-SGM3, NOD *scid* gamma-human SCF/GM-CSF/IL-3; PB, plasmablast(s); PC, plasma cell(s); PSA, passive systemic anaphylaxis; WT, wildtype.

NSG-SGM3 mice were fed autoclaved Teklad Global 18% Protein Extruded Rodent Diet (Inotiv Inc.) (Supplementary Table S1) and received enrofloxacin (Baytril; Elanco US Inc) in sterile drinking water as prophylaxis against opportunistic infections. WT mice were housed in normal rodent housing and treated with untreated filtered drinking water. WT and non-engrafted NSG-SGM3 mice were age-matched with 20–24-week-old engrafted NSG-SGM3 mice at the start of culture experiments. All animal protocols were conducted under the approval and regulation of the Institutional Animal Care and Use Committee at Johns Hopkins University School of Medicine.

2.2 Mouse whole blood and serum samples

For murine whole blood samples, whole blood was collected by retroorbital bleeds into purple-cap Microtainer Tubes containing EDTA (BD Biosciences) at room temperature. Samples were lysed twice with 1x multi-species RBC lysis buffer (Invitrogen) in 5 mL polystyrene round-bottom flow cytometry tubes (Corning) at room temperature in the dark and washed with 1x PBS before antibody staining for flow cytometry. For serum samples, murine whole blood was first collected by retroorbital bleeds into serum separator Microtainer Tubes (BD Biosciences). Tubes were allowed to clot at room temperature for at least 30 minutes and centrifuged at 1000 x g for 10 minutes to separate serum. Serum was stored at -20°C until analysis.

2.3 Quantitative antibody and cytokine measurements

The R-PLEX Human IgE assay (Meso Scale Discovery) and the T-PLEX Human Isotyping Panel 1 kit for human IgM, IgG, and IgA (Meso Scale Discovery) were used to detect levels of human antibodies in NSG-SGM3 mouse sera and in supernatants of *ex vivo* splenocyte cultures after 96 hours. Lyophilized wildtype mouse sera reconstituted in 1x PBS (Sigma) and purified mouse IgE (BD Biosciences) were used as controls to ensure lack of cross-reactivity of the human Meso Scale assays with murine antibodies. Human IgE levels from pooled samples of mouse sera were also confirmed using the ImmunoCAP total serum IgE assay (Thermo Fisher Scientific). Cytokine concentrations of NSG-SGM3 mouse sera were measured using R-PLEX kits for SCF, U-PLEX for GM-CSF and IL-3, U-PLEX for human IL-4 and murine IL-4, and a custom V-PLEX kit for human IL-4, IL-6, IL-13, IFN-γ, and TNF-α (all from Meso Scale Discovery). Recombinant human IL-4 (R&D Biosciences) and murine IL-4 (R&D Biosciences) were used as controls to confirm lack of interspecies cross-reactivity of the Meso Scale IL-4 assays. Sample preparation and processing were performed per manufacturer protocol. Processed plates were read on a MESO QuickPlex SQ 120 machine (Meso Scale Discovery).

2.4 Specific IgE profiling

Mouse sera were pooled into three samples from 5–6 mice each for analysis on the Allergy Xplorer 2 ($ALEX^2$) (Macro Array Diagnostics), which quantifies specific IgE antibodies for 295 clinically relevant allergens (19, 20). In brief, samples were diluted 1:5 in an assay diluent containing MUXF, a carbohydrate cross-reactive determinant (CCD)-blocking agent (21). From this, 500 µL of sample was incubated on a chip cassette for two hours. The chip was then washed and incubated with substrate for eight minutes, after which the reaction was stopped. Results were read on the ImageExplorer instrument (Macro Array Diagnostics) and reported in kUA/L following interpolation by Raptor software from a built-in total IgE calibration curve. Levels >0.10 kUA/L were considered positive.

2.5 Splenocyte harvest and *ex vivo* cultures

To harvest and culture bulk *ex vivo* splenocytes, we modified published protocols originally designed for the harvest and *ex vivo* cultures of $CD19^+$ B cells (22, 23). Briefly, spleens of WT, non-engrafted NSG-SGM3, or engrafted NSG-SGM3 mice were harvested and mashed through a 70 µm cell strainer (Corning Life Sciences) into a 6-well flat-bottom plate containing RPMI-1640 media (Corning) supplemented with 2.05 mM L-glutamine (DiagnoCine Precision), 15% fetal calf serum (Sigma Aldrich), 1% penicillin and streptomycin (Gibco), and 50 µM 2-mercaptoethanol (Sigma). Cells were spun at 500 x g for five minutes at room temperature. Erythrocytes were then lysed with 1x multi-species RBC lysis buffer (Invitrogen) and remaining bulk splenocytes were washed and spun.

Harvested bulk WT, non-engrafted NSG-SGM3, or engrafted NSG-SGM3 splenocytes were initially plated in 6-well flat-bottom plates at 1 x 10^6 cells/mL in supplemented RPMI media as above, and incubated from 0 to 48 hours with either 1 µg/mL mouse anti-human CD40 monoclonal antibody (anti-hCD40; BD Pharmingen) and 10 ng/mL recombinant human IL-4 (hIL-4; R&D Systems) anti-human stimulatory cytokines, or 1 µg/mL hamster anti-mouse CD40 monoclonal antibody (anti-mCD40; BD Biosciences) and 10 ng/mL recombinant mouse IL-4 (mIL-4; R&D Systems) anti-mouse stimulatory cytokines. At 48 and 72 hours, cells were replated in 12-well flat-bottom plates at 1 x 10^6 cells/mL in fresh supplemented RPMI media and re-incubated at both timepoints with the appropriate anti-human or anti-mouse stimulatory cytokines at 0.5 µg/mL CD40L and 5 ng/mL IL-4 concentrations. Culture supernatants were obtained at the 96-hour timepoint and stored at -20°C until further analysis using MSD Multiplexing kits as above (Meso Scale Discovery). Cultures were maintained in a 37°C incubator at 5% CO_2 for 96 hours total before harvest.

2.6 Human donor whole blood samples

Human whole blood samples were obtained from healthy donors consented under a protocol approved by the Institutional Review Board at Johns Hopkins University School of Medicine. Human whole blood samples were collected via standard phlebotomy and drawn into purple-cap BD Microtainer blood collection tubes containing EDTA (BD Biosciences) prior to preparation. Samples were lysed with 1x multi-species RBC lysis buffer (Invitrogen) in 5 mL polystyrene round-bottom flow cytometry tubes (Corning) at room temperature in the dark and then washed with 1x PBS before proceeding with antibody staining for flow cytometry.

2.7 Flow cytometry and analysis of *ex vivo* cultures and whole blood samples

Antibody and miscellaneous reagent concentrations for flow cytometry were titrated based on manufacturer protocols (Supplementary Table S2).

For the preparation of *ex vivo* splenocyte cultures at 0 hour or 96 hour timepoints, harvested cells were washed with 1x PBS, assessed for viability using LIVE/Dead Fixable Aqua (Invitrogen), incubated with a blocking cocktail containing rat anti-mouse CD16/CD32 (mouse BD Fc block; BD Biosciences), human BD Fc Block (BD Biosciences), and True-Stain Monocyte Blocker (BioLegend), and subsequently stained with 100 µL of either anti-human or anti-mouse antibody cocktail (Supplementary Table S2). For preparation of human donor and mouse whole blood, RBC-lysed and washed cells were assessed for viability using LIVE/Dead Fixable Aqua, incubated with a blocking cocktail containing human BD Fc block and True-Stain Monocyte Blocker, and subsequently stained with 100 µL of either anti-human or anti-mouse antibody cocktail (Supplementary Table S2). All stained mouse and human samples were fixed in 50 µL 4% paraformaldehyde in 1x PBS and stored at 4° C until time of analysis. Fixed and stored samples were resuspended in 150 µL 1x PBS immediately prior to cytometer analysis. UltraComp eBeads (Invitrogen), ArC amine reactive beads (Invitrogen), and ArC amine negative beads (Invitrogen) were utilized per manufacturer protocol for compensation of the appropriate antibodies. Samples were run on a Cytek Aurora cytometer (Cytek Biosciences).

Flow cytometry samples were analyzed on FlowJo v10 software (Tree Star) using gating strategies specifically designed to exclude follicular, marginal zone, and germinal center B cells that may otherwise contribute to false positive signal from the final gate (Supplementary Figures S1, S2). Specifically, human PC were identified by gating sequentially on singlet, live, human $CD138^+$ human $CD19^{var}$, human IgD^-, human $CD23^-$, human $CD138^+$ human $CD27^+$ cells (Supplementary Figure S1). Human MBC were gated sequentially on singlet, live, human $CD19^+$ human $CD138^-$, human IgD^-, human $CD23^-$, human $CD20^+$ human $CD27^{+/hi}$ cells (Supplementary Figure S1). Mouse PC and PB were gated sequentially on singlet, live, mouse $CD138^{hi}$, mouse IgD^- mouse $CD22^-$, mouse/human GL-7^{lo}, mouse/human $B220^{lo}$ cells; thereafter, mouse PC were gated as mouse $CD138^+$ mouse $CD19^+$ cells, and mouse PB were gated as mouse $CD138^+$ mouse $CD19^-$ cells (Supplementary Figure S2). Mouse MBC were gated sequentially on singlet, live, mouse $CD138^-$, mouse IgD^- mouse $CD22^-$, mouse/human GL-7^{lo}, mouse $CD273^+$ mouse/human $B220^+$ cells (Supplementary Figure S2). Minimal cross-reactivity between anti-human and anti-murine antibodies with murine and human samples, respectively, were validated using murine whole blood, murine splenocytes, and human donor whole blood (Supplementary Figure S3).

2.8 *In vivo* systemic anaphylaxis

Anaphylaxis experiments were performed at least 16 weeks post-engraftment. For direct targeting of IgE, engrafted and non-engrafted NSG-SGM3 mice were injected intraperitoneally with 100 ng or 1 µg of goat polyclonal anti-human IgE (Hybridoma Reagent Laboratory) or equivalent amounts of normal polyclonal goat IgG isotype control (R&D Systems) diluted in sterile 1x PBS. To assess anaphylaxis responses, core body temperature was measured using a rectal probe (Kent Scientific), and clinical score was assessed every ten minutes over the course of one hour. Clinical scores from zero to five were as follows: 0) asymptomatic; 1) scratching; 2) piloerection, facial edema, 3) labored breathing, reduced activity; 4) coma or unresponsiveness; and 5) death. In the event of death, temperature measurements for that specific mouse were terminated.

For planned food challenges, enough blood was obtained from two engrafted NSG-SGM3 mice to allow for full specific IgE profiling of their individual sera on the $ALEX^2$ chip. While numerous low-level positives were noted, consistent with the previously described pooled samples, both mice had specific IgE antibodies to several foods, of which three foods were selected for challenges based on ease of administration via oral gavage and lack of prior exposure to these allergens. Mice were challenged by oral gavage with 200 µL nonfat cow's milk (corresponding to 6.6 mg protein; Whole Foods), 20 mg yeast dissolved in water (11.3 mg protein; Anthony's Brewer's Yeast Powder), and 56 mg hazelnut paste diluted in water (8.3 mg protein; Pariani Unsweetened Hazelnut Paste) in separate experiments. Anaphylaxis responses were assessed as described above.

2.9 Basophil activation testing

Human blood samples were obtained from healthy volunteer donors after informed consent under an Institutional Review Board-approved protocol. Blood was collected via standard phlebotomy and drawn into 4 mL lithium heparin phlebotomy tubes (BD Biosciences). Whole blood was incubated for 30 minutes at 37°C with goat polyclonal anti-human IgE (Hybridoma Reagent Laboratory), polyclonal goat IgG isotype control (R&D Systems), or 1 µM N-formylmethionyl-leucyl-phenylalanine (Sigma), diluted in PAGCM buffer containing piperazine-N,N′-bis[2-ethanesulfonic

acid], bovine serum albumin (MP Biomedicals), glucose (Sigma-Aldrich), 1.7 mM calcium (Sigma), and 1.7 mM magnesium (Sigma). After stimulation, cells were fixed with BD Phosflow Fix Buffer (BD Biosciences), centrifuged for five minutes at 400 x g, and resuspended in Pipes buffer containing 1 mM EDTA and 0.25% bovine serum albumin.

In preparation for analysis, cells were blocked with 1 mg/mL non-specific human IgG (MB Biological), incubated with fluorescently-conjugated monoclonal anti-human CD63 (1:1000 dilution; BD Pharmingen) and anti-human FcεRIα (clone CRA-1, 1:250, Life Technologies) antibodies at room temperature for 25 minutes, and then stained with secondary antibodies anti-CD123-PE (1:100, BD Biosciences), anti-mouse IgG2b-AlexaFluor488 (1:1000, Life Technologies), and anti-mouse IgG1-AlexaFluor647 (1:1000, Life Technologies) at room temperature for 25 minutes. Samples were analyzed on a BD Accuri C6 flow cytometer (BD Biosciences) using a previously-defined gating strategy (24). The percentage of $CD63^+$ basophils was recorded for each sample.

2.10 Quantification and statistical analysis

Each datapoint represents one sample from one mouse and error bars represent SEM in Figures 1–3 unless otherwise stated. Data and error bars in Figure 4 represent mean ± SEM unless otherwise stated. Statistical analyses were determined by unpaired Student's *t*-test or two-way ANOVA with post-hoc Šídák's multiple comparisons test (full model mixed-effects analysis), as specifically denoted in the figure captions and applied based on experimental design. P-values < 0.05 were considered statistically significant. Statistical tests and plotting were performed using GraphPad Prism 10 (GraphPad Software, Inc).

3 Results

3.1 Naïve engrafted NSG-SGM3 mice produce abundant circulating human antibodies, including IgE, in the absence of active sensitization

The sera of NSG-SGM3 mice were first analyzed for human antibody titers, demonstrating that naïve engrafted NSG-SGM3 mice without prior marrow ablation produced easily detectable quantities of human IgM, IgG, IgA, and IgE antibodies without active sensitization to antigens, as compared to no detectable amounts from non-engrafted NSG-SGM3 or wildtype C57BL/6J (WT B6) controls (Figure 1A). Similar concentrations of serum total IgE were seen within batches of NSG-SGM3 mice engrafted with the same donor HSCs, and IgE concentrations also correlated better by donor HSC than by engraftment efficiency determined by circulating human $CD45^+$ count. Of note, even the lowest IgE levels were remarkably several-fold more abundant than that of the average human patient (typically below 200–240 ng/mL for healthy non-atopic humans) (25, 26), while the levels of human IgM, IgG, and IgA were sub-physiologic by several folds (27–29). These human antibody concentrations highlight basal human antibody production in our naïve and otherwise unsensitized humanized mice raised in specific-pathogen free facilities.

We next investigated the landscape of circulating human cytokines, particularly those necessary for human B cell antibody class switching. NSG-SGM3 mice exhibited comparable serum levels of human GM-CSF and IL-3 regardless of the presence or absence of HSC engraftment or the efficiency of HSC engraftment determined by circulating human $CD45^+$ count (Figure 1B), reflecting constitutive production as previously described (10, 30). NSG-SGM3 mice also produced substantial human SCF (Figure 1B), with engrafted mice expressing similar levels to those previously reported for irradiated NSG-SGM3 BLT mice engrafted with fetal liver-derived HSCs (10). However, only engrafted NSG-SGM3 mice exhibited easily detectable serum levels of human IL-4 and IL-13 (Figure 1C), which are cytokines essential for type II immunity and IgE class switch recombination, as well as physiologic ranges of human Th1 cytokines IL-6, interferon gamma (IFN-γ), and tumor necrosis factor alpha (TNF-α) (Figure 1D) (31–34). Surprisingly, both engrafted and non-engrafted NSG-SGM3 mice produced large amounts of murine IL-4 from residual murine immune cells (Figure 1C). In contrast, WT B6 mice used as controls did not have detectable serum murine IL-4, consistent with prior reports for this mouse strain which is known to produce less IL-4 than other strains due to fewer invariant natural killer T cells (33, 35). These data thus confirm that engrafted human HSCs in NSG-SGM3 mice without prior ablation can differentiate into functional human immune cells that produce human Th2 cytokines to support B cell class switching and IgE production.

3.2 Human IgE from engrafted NSG-SGM3 mice is polyclonal and recognizes a diverse array of allergens

To further profile the functional roles of human IgE produced by humanized NSG-SGM3 mice, we sought to determine the range of allergen specificity of their serum human IgE. We utilized the $ALEX^2$ multiplex chip to test human IgE reactivity to 295 clinically relevant molecular and extract-based allergens, including aeroallergens (e.g. grasses, trees, animal dander), common plant-derived and animal-derived food allergens, and stinging insect venoms. Pooled serum samples from engrafted NSG-SGM3 mice, which again demonstrated considerable total human IgE levels (Figure 1E), revealed a diverse profile of allergen specificities (Table 1; Supplementary Table S3). Low levels of specific IgE antibodies, all below 2 kUA/L, were detected across seven of eight total broad categories of allergens (plant-derived food; animal-derived food; pollen; mite; insect/venom; animal origin; microorganism/spore; other). The highest specific IgE levels observed were either against foods not present in the mouse chow diet (Supplementary Table S1) or against allergens otherwise highly unlikely to be encountered in the specific-pathogen free mouse

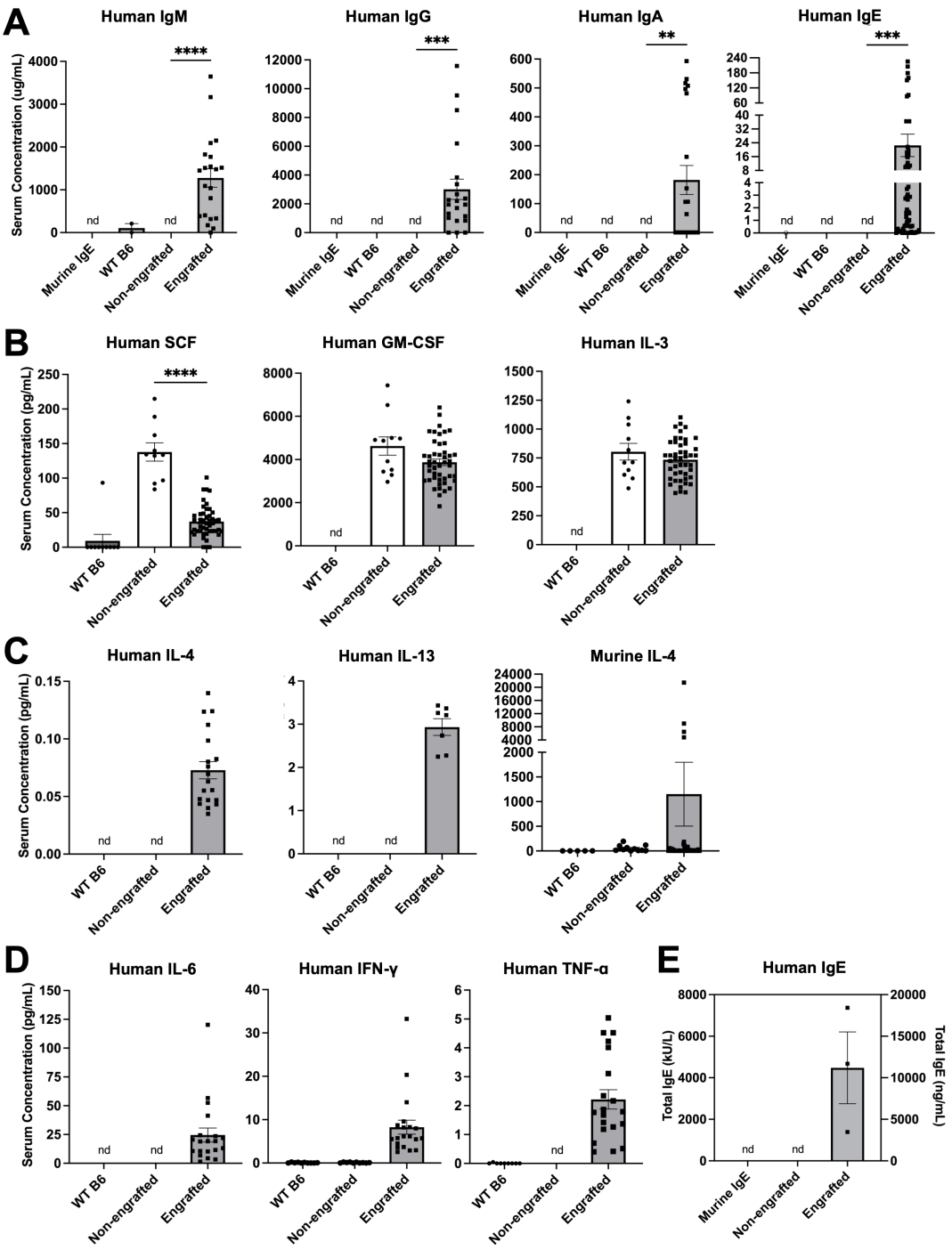

FIGURE 1
Engrafted NSG-SGM3 mice spontaneously produce abundant circulating human antibodies, including IgE. **(A)** Serum concentrations of human IgM, IgG, IgA, and IgE antibodies for WT, non-engrafted NSG-SGM3, and engrafted NSG-SGM3 mice. Murine anti-DNP IgE antibody was used as an isotype control (nd = not detectable; *n* = 2 WT, 3 non-engrafted NSG-SGM3, and 22 engrafted NSG-SGM3 mice compiled from two different experiments for IgM, IgG, and IgA; *n* = 14 WT, 7 non-engrafted NSG-SGM3, and 63 engrafted NSG-SGM3 mice compiled from three different experiments for IgE). **(B)** Serum concentrations of human SCF, GM-CSF, and IL-3 cytokines for WT (*n* = 10–11), non-engrafted NSG-SGM3 (*n* = 10–11), and engrafted NSG-SGM3 (*n* = 46) mice. **(C)** Serum concentrations of human IL-4, human IL-13, and murine IL-4 Th2 cytokines for WT (*n* = 5–10), non-engrafted NSG-SGM3 (*n* = 10–11), and engrafted NSG-SGM3 (*n* = 11–37) mice. **(D)** Serum concentrations of human IL-6, IFN-γ, and TNF-α Th1 cytokines for WT (*n* = 10), non-engrafted NSG-SGM3 (*n* = 10–11), and engrafted NSG-SGM3 (*n* = 20) mice. **(E)** Total serum human IgE levels in engrafted versus non-engrafted NSG-SGM3 mice, determined by secondary ImmunoCAP assay from ALEX^2 allergen chip analysis. Murine IgE antibody was used as an isotype control. Values reflect serum concentrations in kU/L (left y-axis) or ng/mL (right y-axis) (*n* = 3 samples pooled from five mice each). Error bars in **(A–E)** represent SEM. P values < 0.05 were considered significant (**p < 0.01; ***p < 0.001; ****p < 0.0001). Welch's *t*-test was used for **(A, B)**.

facility environment, including millet *Pan m* (0.17–1.35 kUA/L), egg yolk *Gal* d_{yolk} (0.13–0.22 kUA/L), cashew *Ana o* (0.22–0.26 kUA/L), and cottonwood (0.71–0.83 kUA/L) (Table 1; Supplementary Table S3). This diverse and broad range of allergen specificities therefore suggests that even without deliberate active sensitization, NSG-SGM3 mice produce low basal levels of functional polyclonal human IgE specific to diverse allergens, likely including numerous others not tested for by the $ALEX^2$ chip, as opposed to one monoclonal IgE antibody specific to a singular allergen.

3.3 Human CD40L and IL-4 expand human plasma cells and memory B cells in engrafted NSG-SGM3 splenocytes *ex vivo*

Next, we aimed to validate whether NSG-SGM3 mice can support the differentiation and maturation of engrafted human $CD34^+$ HSCs into human IgE-producing B cells. We first stimulated splenocytes from engrafted NSG-SGM3, non-engrafted NSG-SGM3, or WT B6 mice *ex vivo* using either human or murine stimulatory CD40L and IL-4 cytokines (Figure 2A) (22, 23). We then analyzed cells by flow cytometry for the expansion of human versus murine plasma cells (PC) and memory B cells (MBC) (Supplementary Figures S1-S3) (18, 36–39).

As compared to WT splenocytes, engrafted NSG-SGM3 splenocytes stimulated with human CD40L and IL-4 cytokines *ex vivo* for 96 hours exhibited a significantly increased percentage of human $CD138^+$ $CD27^+$ cells, indicating relative enrichment of antibody-producing human PC (Figure 2B). While there was mild but non-significant expansion of human PC in response to murine cytokines (Figure 2B), suggestive of low/minimal interspecies cross-reactivity, human IgE antibodies were detected in the culture supernatants of only engrafted NSG-SGM3 splenocytes stimulated with human (but not murine) cytokines (Figure 2C). In contrast, the percentage of murine PC and younger plasmablasts (PB) in response to human or mouse stimulatory cytokines was similar between engrafted NSG-SGM3 mice and WT mice (Figure 3A). Notably, non-engrafted NSG-SGM3 splenocytes were poor controls for flow cytometry due to significant autofluorescence at baseline and high cell death during splenocyte harvest and throughout *ex vivo* culture, which contributed to significant non-specific and falsely positive fluorescent signal (Supplementary Figure S4). Even so, the undetectable levels of human IgE from culture supernatants of non-engrafted NSG-SGM3 mice stimulated with human or murine cytokines suggest that human IgE-secreting PC were not expanded (Figure 2C), as expected given their lack of engrafted human HSCs. Therefore, engrafted NSG-SGM3 mice harbor a Th2 cytokine-responsive population of human PC that can secrete human IgE.

Consistent with our PC findings, engrafted NSG-SGM3 stimulated with human cytokines also exhibited an increase in the percentage of human $CD20^+$ $CD27^+$ cells as compared to WT splenocytes, which reflects expansion of human MBC (Figure 2D), despite comparable percentages of murine MBC (Figure 3B). In addition, at baseline prior to *ex vivo* culture, human PC and MBC were detected in engrafted NSG-SGM3 mice, albeit at rare and low percentages, but were undetectable in WT splenocytes (Figure 2E). In contrast and as expected, at baseline prior to culture, engrafted NSG-SGM3 mice had a comparable percentage of murine PC/PB and mildly decreased percentage of murine MBC as compared to WT mice (Figure 3C). These data are suggestive of the presence of rare and possibly resting or lowly-active maintenance populations of human PC and MBC in engrafted NSG-SGM3 mice, which can expand upon Th2 cytokine stimulation even with present residual murine immune cells. Our *ex vivo* findings also support our data on abundant human antibody production in naïve engrafted NSG-SGM3 mice (Figure 1A), by highlighting putative upstream human HSC-derived cells which can mature into and expand human PC and MBC populations in response to Th2 cytokines to help sustain the production of basal human IgE.

3.4 Engrafted NSG-SGM3 mice can undergo anaphylaxis following administration of anti-human IgE antibody but not by challenge with food allergen

Lastly, we explored the functionality of human IgE produced by engrafted NSG-SGM3 mice. To understand the anaphylaxis-inducing potential of the polyclonal human IgE and confirm binding of this human IgE to surface FcεRI receptors on human mast cells and basophils, we utilized a one-step model involving systemic challenge with a single dose of goat anti-human IgE antibody. Remarkably, a single intraperitoneal injection of this goat IgG specific to human IgE into engrafted NSG-SGM3 mice induced a significant dose-dependent decrease in core body temperature and increase in anaphylaxis clinical scores (Figure 4A). In contrast, non-engrafted NSG-SGM3 mice given anti-human IgE and engrafted NSG-SGM3 mice given goat IgG isotype control did not exhibit clinical reactivity (Figure 4A). We further confirmed the lack of interspecies binding of goat IgG to murine or human Fcγ receptors using *in vitro* basophil activation assays (Figure 4B). As murine FcεRI receptors cannot bind human IgE (40), our data demonstrate that the polyclonal human IgE produced by humanized NSG-SGM3 mice is physiologically functional and can induce human cell-dependent type I hypersensitivity responses such as anaphylaxis by direct targeting.

We further investigated whether engrafted NSG-SGM3 mice with low levels of food allergen-specific IgE antibodies could undergo anaphylaxis in response to specific food allergen challenge. Engrafted NSG-SGM3 mice did not exhibit clinical reactivity after oral gavage with cow's milk (serum anti-Bos d 4-IgE of 0.13 and 0.31 kUA/L, respectively), yeast (anti-Sac c-IgE of 0.43 and 0.65), or hazelnut (anti-Cor a 11-IgE of 0.19 and 0.41) (Figure 4C). Together, these data suggest that human IgE in humanized NSG-SGM3 mice do harbor functional Fc receptors but, at least with such low levels of food-specific IgE, are not able to elicit clinical anaphylaxis by oral challenge with food allergen.

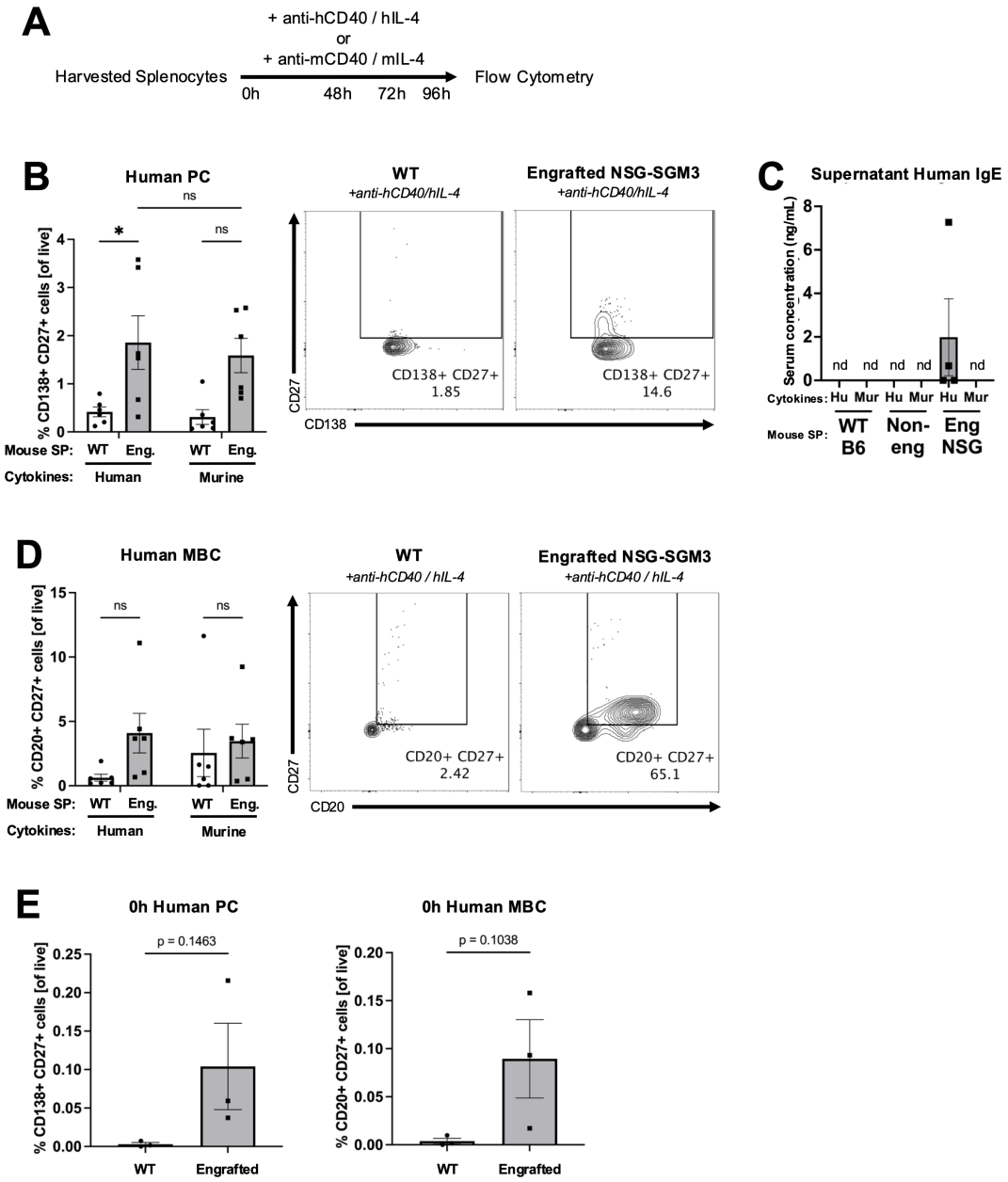

FIGURE 2
Human plasma cells and memory B cells expand from engrafted NSG-SGM3 splenocytes cultured with human Th2 cytokines *ex vivo*.
(A) Experimental design for assessing *ex vivo* expansion of human and murine plasma cells (PC) or memory B cells (MBC) from bulk splenocytes (SP). Harvested splenocytes were cultured with anti-human CD40 and human IL-4 cytokines (anti-hCD40/hIL-4) or anti-murine CD40 and murine IL-4 cytokines (anti-mCD40/mIL-4) for 96 hours (h). **(B)** Percentage of and representative flow cytometry plots for $CD138^+$ $CD27^+$ human PC (of all live) from WT (circle) versus engrafted NSG-SGM3 ("Eng."; square/gray) splenocytes cultured for 96 hours with either human or murine cytokines. Values were calculated using cell counts of sequentially gated $CD138^+$ $CD19^{var}$, IgD^-, $CD23^-$, $CD138^+$ $CD27^+$ human PC, divided by all live cells (n = 6 mice/group, compiled from three independent experiments). **(C)** Concentration of human IgE in supernatants of *ex vivo* cultures of WT, non-engrafted NSG-SGM3, or engrafted NSG-SGM3 splenocytes cultured with either human or murine cytokines (n = 4 mice/group). **(D)** Percentage of and representative flow cytometry plots for $CD20^+$ $CD27^+$ human MBC (of all live) from WT versus engrafted NSG-SGM3 (square/gray) splenocytes cultured for 96 hours with either human or murine cytokines. Values were calculated using cell counts of sequentially gated $CD19^+$ $CD138^-$, IgD^-, $CD23^-$, $CD20^+$ $CD27^+$ human MBC, divided by all live cells (n = 6 mice/group, compiled from three independent experiments). **(E)** Baseline percentage of human PC and MBC for WT versus engrafted NSG-SGM3 (square/gray) splenocytes at zero hours prior to *ex vivo* culture. Values were calculated as discussed in **(B, D)** (n = 4 mice/group, compiled from two independent experiments). Error bars in **(B–E)** represent SEM. P values < 0.05 were considered significant (*p < 0.05; ns, not significant). Two-way ANOVA with post-hoc Šídák's multiple comparisons test (full model mixed-effects analysis) was used for **(B, D)**, and unpaired Student's t-test was used for **(E)**. See Supplementary Figures S1-S3 and Supplementary Table S2 for additional details on gating strategy and antibody staining for flow cytometry (SP, splenocytes; Hu, human cytokines, Mur, murine cytokines).

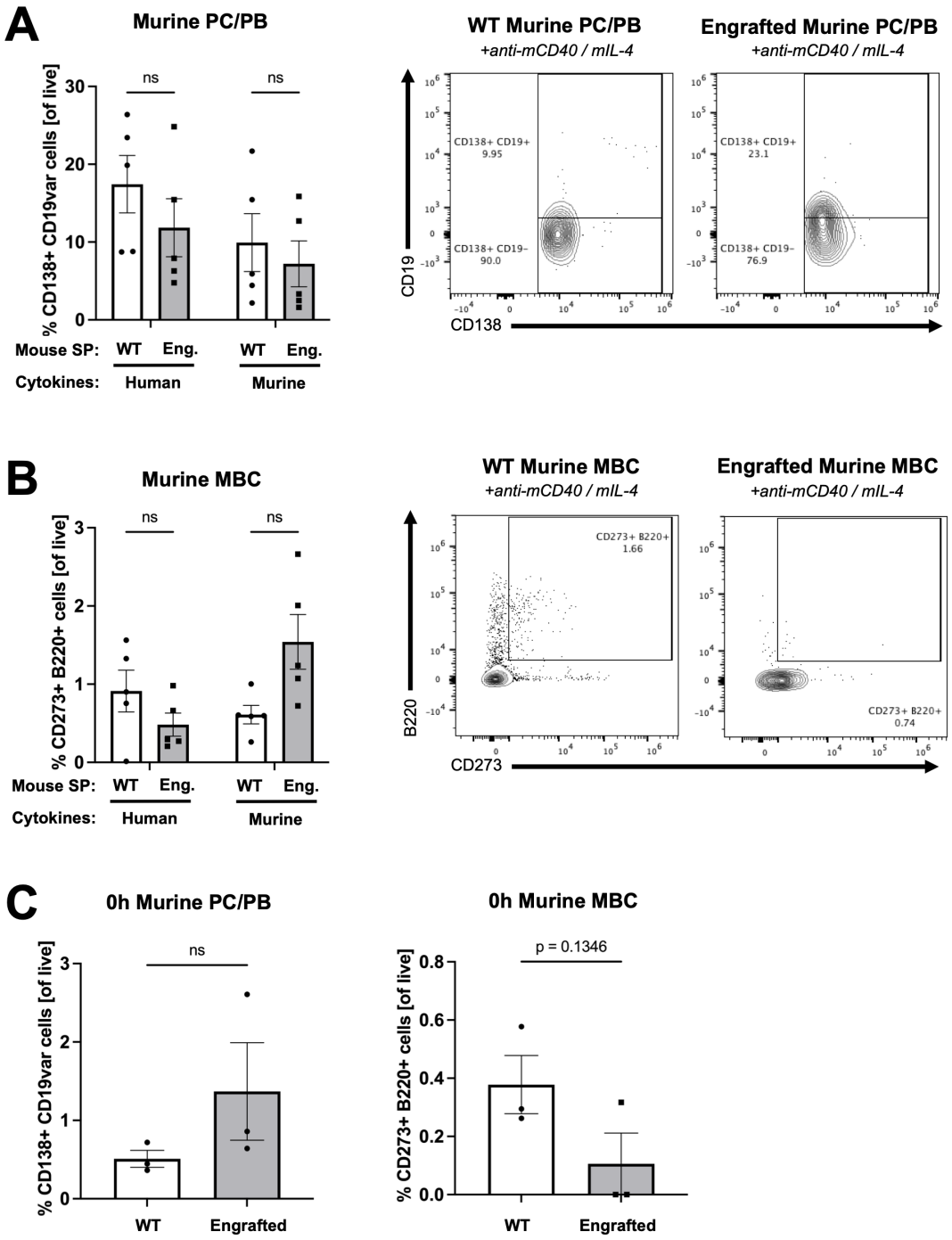

FIGURE 3
Human B cells demonstrate minimal expansion from engrafted NSG-SGM3 splenocytes cultured with murine cytokines *ex vivo*. **(A)** Percentage of and representative flow cytometry plots for CD138^{+} B220^{lo} murine PC and plasmablasts (PB) (of all live) from WT versus engrafted NSG-SGM3 ("Eng."; square/gray) splenocytes (SP) cultured for 96 hours with either human or murine cytokines. Values were calculated using cell counts of sequentially gated CD138^{+}, IgD^{-} CD22^{-}, GL-7^{lo}, B220^{lo} murine PC (CD19$^{+/hi}$) plus PB (CD19$^{lo/-}$) cells, divided by all live cells (n = 6 mice/group, compiled from three independent experiments). **(B)** Percentage of and representative flow cytometry plots for CD273^{+} B220^{+} murine MBC (of all live) from WT versus engrafted NSG-SGM3 (square/gray) splenocytes cultured for 96 hours with human or murine cytokines. Values were calculated using cell counts of sequentially gated CD138^{+}, IgD^{-} CD22^{-}, GL-7^{lo}, CD273^{+} B220^{+} murine MBC, divided by all live cells (n = 6 mice/group, compiled from three independent experiments). **(C)** Baseline percentage of murine PC/PB and MBC for WT versus engrafted NSG-SGM3 (square/gray) splenocytes at zero hours prior to *ex vivo* culture. Values were calculated as discussed in **(A, B)** (n = 4 mice/group, compiled from two independent experiments). Error bars represent SEM. P values < 0.05 were considered significant (ns, not significant). Two-way ANOVA with post-hoc Šídák's multiple comparisons test (full model mixed-effects analysis) was used for **(A, B)**, and unpaired Student's t-test was used for **(C)**. See Supplementary Figures S1-S3 for additional details on gating strategy and antibody staining for flow cytometry (SP, splenocytes).

4 Discussion

We herein demonstrate that humanized NSG-SGM3 mice engrafted with human HSCs spontaneously produce all human antibody isotypes (Figure 1A), even without prior marrow ablation or human lymphoid tissue implantation. To our knowledge, this is the first report that NSG-SGM3 mice can produce human IgE (Figures 1A, E). This is consistent with prior reports of human IgM and IgG production in BLT mice and NSG-SGM3 mice engrafted after irradiation (4, 18). Furthermore, we demonstrate that the human IgE is polyclonal and recognizes a diverse set of allergens (Table 1; Supplementary Table S3). This finding further highlights how human HSC engraftment alone is actually "self-sufficient" to generate human Th2 cytokines needed for human IgE production despite a still-present residual murine background (Figure 1C). Thus, our novel findings characterize the spontaneous production of a polyclonal IgE repertoire in an otherwise unsensitized NSG-SGM3 humanized mouse.

Additionally, we identify putative human $CD138^+$ $CD27^+$ plasma cell and $CD20^+$ $CD27^+$ memory B cell populations expanded by Th2 cytokines to facilitate IgE secretion (Figures 2B–D), offering a novel humanized mouse model for the study of human IgE B cell biology. As human PC and MBC tend to reside in lymphoid structures (41), it is perhaps surprising that an unablated NSG-SGM3 mouse with only murine lymphoid structures can adequately support human B cell survival and differentiation from engrafted human HSCs, let alone functional human IgE production. In addition to human Th2 cytokines, other cross-reactive signals impacting human PC and MBC expansion are likely also released *in vivo* by host murine lymphoid and stromal tissues, even if differences in mouse and human lymphoid organ structure or cellular composition are driving different signaling molecule repertoires. Of note, our culture model using bulk splenocytes rather than purified B cells may better capture the full spectrum of cross-reactive murine signals such as pro-apoptotic factors (Figure 2A), given that human PC and MBC were indeed detected from engrafted NSG-SGM3 mice (Figures 2B–D). Additional homing sites in other murine lymphoid tissues may also exist. It would be interesting to characterize the trafficking patterns of human PC and MBC and any differing murine-derived signaling factors in our NSG-SGM3 model as compared to traditional BLT mice. This is likely difficult to study, however, especially as IgE^+ B cells are exceedingly rare and thus difficult to track without IgE-inducing triggers such as allergen sensitization, glucocorticoid exposure, or germ-free diet from a young age (23, 39, 42).

It is also of interest to consider the source and physiologic implications of IgE memory in our model. As our humanized NSG-SGM3 mice produce basal polyclonal IgE found in blood and presumably also bound to FcεRI receptors on mast cells and basophils (Figure 1A and 4A), there is likely constant low-level repopulation of multiple clones of human IgE-secreting cells to maintain basal secretion of polyclonal IgE. Data on the source of IgE memory in humans favor a population of IgG MBC which can re-differentiate into IgG plasma cells and subsequently class switch to and secrete IgE (39, 41, 43–50), though human IgE^+ MBC that directly re-differentiate into IgE-secreting PC may also exist (51, 52). The former hypothesis is bolstered by data showing that chronic IgE B cell receptor signaling is self-constraining, which not only regulates IgE production by intrinsically restricting the lifespans of IgE^+ B cells and PC, but likely also prohibits differentiation into IgE^+ MBC (46–48, 50). While we demonstrated human IgE secretion by engrafted NSG-SGM3 splenocytes stimulated *ex vivo* with Th2 cytokines (Figure 2C), the signaling kinetics of and the downstream impact on human B cell maturation *in vivo* for IgE^+ B cell receptors specifically still need to be explored.

Additionally, given that older NSG-SGM3 mice can develop HLH/MAS-like pancytopenia (14–17), a component of inadequate or even absent immune regulation may be involved in priming these mice for IgE production. Although irradiated and engrafted NSG-SGM3 mice have increased functional regulatory T cells (10), gut dysbiosis in the setting of a murine-immunodeficient host or other factors known to drive high IgE levels in mice could further contribute to these human IgE levels above typical non-atopic levels (23, 42, 53, 54). Further investigations into cell-cell circuits and other physiologic and/or immune regulatory states affecting human IgE production and functionality in NSG-SGM3 mice and other humanized mouse models are warranted.

One limitation of our work includes the fact that we have not identified that human IL-4 is necessary for production of human IgE, for example by administering an anti-IL-4 blocking antibody. Furthermore, the exact cellular sources of human IL-4 presumably driving human IgE class switching in our model remain unclear. The most likely candidates are human basophils, which are greatly expanded in response to high levels of IL-3, SCF, and GM-CSF from the human transgenes (8). Other possible but likely minor contributors include human T follicular helper cells (Tfh) and type II innate lymphoid cells (ILC2). On the other hand, murine IL-4, which is secreted by residual murine granulocytes in NSG-SGM3 mice (8), is thought to be species-specific and not cross-reactive for human B cells (55, 56). In line with this, our *ex vivo* data clearly demonstrate that murine Th2 cytokines do not significantly expand human $CD138^+$ $CD27^+$ PC and $CD20^+$ $CD27^+$ MBC (Figures 2B, D) or drive IgE production (Figure 2C) in engrafted NSG-SGM3 splenocytes. Though low cross-reactivity from murine IL-4 cannot be fully ruled out, the effects are likely minimal and human IL-4 remains as the most likely driving signal of human IgE production in humanized NSG-SGM3 mice.

We also demonstrate that the NSG-SGM3 basal IgE repertoire recognizes an array of human-relevant allergens despite the lack of intentional active allergen sensitization (Table 1; Supplementary Table S3). These low specific IgE titers likely reflect low-level sensitization without allergic reactivity, given that the mice do not appear to react to food allergen epitopes. Although anaphylaxis was induced by cross-linking IgE directly via administration of anti-human IgE antibody (Figure 4A), no clinical reactivity was observed during oral challenge with multiple food allergens to which the mice had never before been exposed (Figure 4C). This lack of clinical reactivity could be due to the very low specific IgE titers, often in the range of 0.1-0.3 kUA/L, which are below the typical clinical cut-off

of 0.3 kUA/L for diagnostics in humans. For a small subset of food allergens, such as wheat and soy, it is possible that the presence of these foods in the daily diet of these mice (Supplementary Table S1) may have induced a desensitized state. Of note, however, we only tested three easily accessible food allergens for oral allergen challenge, and additional reactive allergens of clinical significance may not have been captured within the 295 tested allergens (Supplementary Table S3). Still, these low titers could reflect the observation that many human patients also produce basal polyclonal serum IgE to various allergens without symptomology upon exposure (57–59).

However, the full mechanism behind the production and function of this polyclonal IgE is still unclear. Of note, our humanized mice were introduced to mouse chow in young adulthood prior to engraftment and also received multipotent human HSCs rather than differentiated B cells. As the positive allergen-specific IgE titers varied between samples, which were pooled from mice receiving different donor HSCs, it is possible that features specific to each donor patient could dictate the particular repertoire of allergen specificities. For example, epigenetic programming of donor patient HSCs prior to extraction (60–63), perhaps in response to real-world or *in utero* allergen exposures or other immunomodulatory signals (e.g. from gut microbiota) sustained earlier by the donor patient (42, 62, 64), may potentially skew the clonality of the IgE repertoire, though this is not well-studied. Other mechanisms modulating IgE function may also be involved. For example, the anaphylactic capacity of IgE can be altered by glycosylation modifications (65–67). Widespread expression of the low-affinity IgE receptor CD23 on abundant immune cells can also act like an IgE "sink" to mildly alter IgE

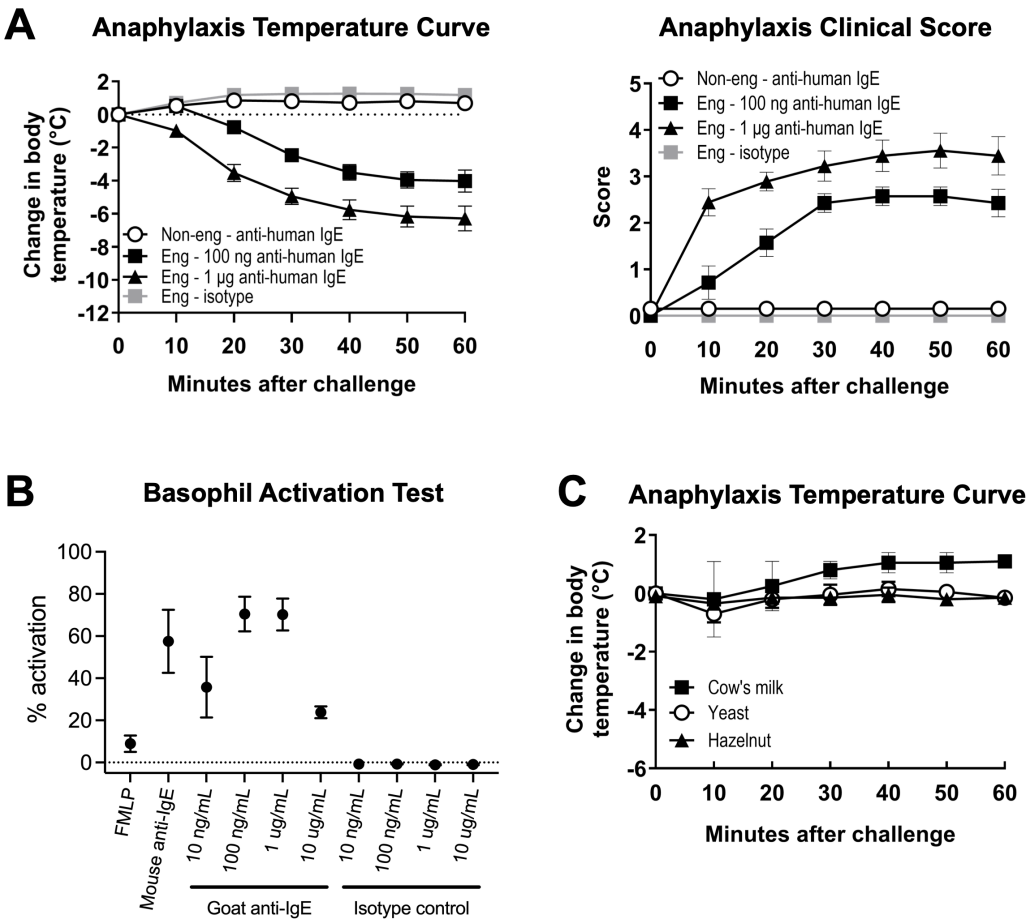

FIGURE 4
Engrafted NSG-SGM3 mice can undergo anaphylaxis with anti-human IgE alone but not by oral challenge with food allergen. **(A)** Change in body temperature (left panel) and clinical scores (right panel) as measures of passive systemic anaphylaxis (PSA) in engrafted NSG-SGM3 mice ("Eng") challenged with 100 ng anti-human IgE (black squares), 1 µg anti-human IgE (black triangles), or equivalent doses of isotype control (gray squares), versus non-engrafted NSG-SGM3 mice challenged with the same doses of anti-human IgE ("Non-eng"; white circles). Values represent mean ± SEM (n = 7–14 mice/group, compiled from five independent experiments). Clinical scores range from zero to five as follows: 0) asymptomatic; 1) scratching; 2) piloerection, facial edema; 3) labored breathing, reduced activity; 4) coma or unresponsiveness; and 5) death). **(B)** Percentage of basophil activation for whole blood basophils from healthy human donors activated for 30 minutes with 1 µM FMLP, 1 µg/mL mouse anti-IgE, or indicated concentrations of polyclonal goat anti-human IgE ("Goat anti-IgE") or goat polyclonal IgG isotype control ("Isotype control"). Values represent mean percentage of basophils with upregulated CD63 surface expression by flow cytometry (n = 3 human donors). **(C)** Change in body temperature as measure of systemic anaphylaxis for engrafted NSG-SGM3 mice challenged via oral gavage to foods to which they had positive specific IgE antibodies: cow's milk (black squares), yeast (white circles), and hazelnut (black triangles). All clinical scores for food challenge experiments were 0. Values represent mean ± SEM (n = 2 mice for three foods each). Error bars represent SEM.

10.3389/fimmu.2025.1628194

availability for binding to FcεRI on granulocytes and thus downstream granulocyte function (68–70).

Despite polyclonal reactivity of the human IgE to multiple allergens (Table 1), different IgE antibodies within the NSG-SGM3 IgE repertoire could have variable affinity to their allergen such that some IgE antibodies are individually inadequate to induce anaphylaxis by allergen challenge. Typically, high-affinity anaphylactic IgE is thought to require sequential switching of IgG B cells to IgE B cells in germinal centers for somatic hypermutation and affinity maturation (71, 72). In contrast, lower-affinity and broadly-specific "natural" IgE, produced by direct switching from IgM to IgE B cells without significant affinity maturation (23, 73, 74), is thought to play homeostatic immune roles such as protection from anaphylaxis, cancer surveillance, and skin barrier defenses (23, 75, 76). It is also possible that the polyclonal human IgE repertoire of NSG-SGM3 mice could functionally act like broadly- or non-specific IgE in bulk. This would be consistent with the notion that natural IgE functions in immune protection and surveillance, which may modulate or even compensate in part for the known immune-dysregulated background of NSG-SGM3 mice.

In all, our work uncovers the utility of humanized NSG-SGM3 mice without prior ablation as a humanized mouse model for studying human antibody and B cell biology and for elucidating the physiologic roles of a basal polyclonal antibody repertoire. In particular, this is the first report that naïve NSG-SGM3 mice spontaneously generate polyclonal and functional IgE, which may

TABLE 1 Engrafted NSG-SGM3 mice produce polyclonal human IgE specific to a diverse array of allergens.

Plant food							Animal food						
Type	Subtype	Allergen	E/M	P_1	P_2	P_3	Type	Subtype	Allergen	E/M	P_1	P_2	P_3
Legume	Peanut	Ara h 1	M	≤0.10	≤0.10	0.12	Milk	Camel, milk	Cam d	E	≤0.10	0.36	0.34
		Ara h 8	M	≤0.10	0.12	0.16	Egg	Egg white	Gal d_white	E	0.12	0.12	0.14
	Chickpea	Cic a	E	≤0.10	0.12	0.18		Egg yolk	Gal d_yolk	E	0.13	0.19	0.22
	Soy	Gly m 4	E	≤0.10	0.11	≤0.10	Meat	House cricket	Ach d	E	≤0.10	0.14	0.13
	Lentil	Len c	E	≤0.10	≤0.10	0.14		Rabbit, meat	Ory_ meat	E	≤0.10	≤0.10	0.16
	Cashew	Ana o	E	≤0.10	0.26	0.22	Seafood	Herring worm	Ani s 1	M	0.18	0.16	≤0.10
	Pecan	Car i	E	≤0.10	0.18	0.24	**Pollen**						
	Walnut	Jug r 1	M	≤0.10	0.17	0.23	**Type**	**Subtype**	**Allergen**	**E/M**	**P_1**	**P_2**	**P_3**
		Jug r 6	M	≤0.10	≤0.10	0.17	Grass pollen	Timothy grass	Phl p 1	M	0.23	0.24	0.20
	Maca-damia	Mac inte	E	≤0.10	0.10	0.16		Common reed	Phr c	E	≤0.10	≤0.10	0.16
Seed	Pumpkin seed	Cuc p	E	≤0.10	0.34	0.86	Tree pollen	Tree of heaven	Ail a	E	≤0.10	0.17	0.29
Spice	Paprika	Cap a	E	≤0.10	0.34	0.48		Cypress	Cup a 1	M	≤0.10	≤0.10	0.12
	Parsley	Pet c	E	≤0.10	≤0.10	0.15			Cup s	E	≤0.10	0.25	0.34
Cereal	Oat	Ave s	E	≤0.10	0.17	0.15		Beech	Fag s 1	M	≤0.10	0.10	0.13
	Quinoa	Che q	E	≤0.10	≤0.10	0.16		London plane tree	Pla a 1	M	≤0.10	0.10	0.14
	Common buck-wheat	Fag e	E	≤0.10	0.20	0.25		Cotton-wood	Pop n	E	≤0.10	0.71	0.83
	Barley	Hor v	E	≤0.10	0.21	0.16		Elm	Ulm c	E	≤0.10	0.23	0.34
	Lupine seed	Lup a	E	≤0.10	0.15	0.21	Weed pollen	Russian thistle	Sal k	E	≤0.10	0.17	0.16
	Rice	Ory s	E	0.21	0.28	0.16	**Insect/venom**						
	Millet	Pan m	E	0.17	1.04	1.35	**Type**	**Subtype**	**Allergen**	**E/M**	**P_1**	**P_2**	**P_3**

(Continued)

TABLE 1 Continued

Plant food							Animal food						
Type	Subtype	Allergen	E/M	P_1	P_2	P_3	Type	Subtype	Allergen	E/M	P_1	P_2	P_3
	Cultivated rye	Sec c_flour	E	≤0.10	0.15	0.22	Wasp venom	Paper wasp venom	Pol d	E	≤0.10	0.22	0.18
	Wheat	Tri a 19	M	0.11	0.13	0.21		Wasp venom	Ves v	E	≤0.10	0.13	≤0.10
Fruit	Kiwi	Act d 1	M	≤0.10	0.28	0.40	**Mite**						
		Act d 2	M	≤0.10	0.22	0.19	**Type**	**Subtype**	**Allergen**	**E/M**	**P_1**	**P_2**	**P_3**
Vegetable	Onion	All c	E	≤0.10	0.18	0.21	House dust mite	European house dust mite	Der p 7	M	≤0.10	0.15	≤0.10
	Potato	Sol t	E	≤0.10	0.12	0.19			Der p 21	M	≤0.10	0.11	≤0.10
Microorganism/Spore							Storage mite	Blomia tropicalis	Blo t 5	M	≤0.10	0.17	≤0.10
Type	**Subtype**	**Allergen**	**E/M**	**P_1**	**P_2**	**P_3**			Blo t 10	M	0.10	≤0.10	≤0.10
Yeast	Yeast	Sac c	E	0.15	0.10	0.11		Glycy-phagus domesticus	Gly d 2	M	≤0.10	0.18	0.14
Other							**Legend**						
Type	**Subtype**	**Allergen**	**E/M**	**P_1**	**P_2**	**P_3**	Negative/Uncertain		≤0.10 kUA/L		Moderate IgE		1-5 kUA/L
Latex	Latex	Hev b 3	M	≤0.10	≤0.10	0.10	Very low IgE		0.10-0.30 kUA/L		High IgE		5-15 kUA/L
Ficus	Weeping fig	Fic b	E	0.10	0.23	≤0.10	Low IgE		0.30-1 kUA/L		Very high IgE		> 15 kUA/L

List of positive (>0.10 kUA/L) molecular and extract-based allergen specificities of engrafted NSG-SGM3-produced human IgE. Individual allergens are clustered hierarchically under broad allergen categories and types. Numbers indicate serum human IgE (kUA/L) for three pooled samples of five engrafted NSG-SGM3 mice each (P_1, P_2, P_3), as determined by ALEX^2 ELISA-based IgE multiplex assay. Cutoffs for IgE concentration and severity levels/categories follow the default cutoffs listed for the standard ALEX^2 chip analysis, with positive signal for very low IgE level >0.10 kUA/L as such: white, negative/uncertain IgE level (≤0.10 kUA/L); light yellow, very low IgE (0.10-0.30 kUA/L); green-yellow, low IgE (0.30-1 kUA/L); green, moderate IgE (1-5 kUA/L); dark green, high IgE (5-15 kUA/L); black, very high IgE (>15 kUA/L) (E, allergen extract; M, recombinant molecular allergen).

reflect in part why many human subjects have basal levels of allergen-specific IgE without significant clinical reactivity. Our data also reveal additional novel insights into the dynamics of human B cell maturation, differentiation, and proliferation, in particular for Th2 cytokine-responsive lymphocytes that can facilitate the maintenance of a basal and polyclonal IgE repertoire even without prior sensitization.

Data availability statement

The raw data supporting the conclusions of this article will be made available by the authors, without undue reservation.

Ethics statement

The studies involving humans were approved by Johns Hopkins University School of Medicine Institutional Review Board (IRB). The studies were conducted in accordance with the local legislation and institutional requirements. The participants provided their written informed consent to participate in this study. The animal study was approved by Johns Hopkins University School of Medicine Institutional Animal Care and Use Committee (IACUC). The study was conducted in accordance with the local legislation and institutional requirements.

Author contributions

EL: Data curation, Formal analysis, Investigation, Methodology, Validation, Visualization, Writing – original draft, Writing – review & editing, Conceptualization. RK-B: Conceptualization, Methodology, Writing – review & editing, Data curation, Formal analysis, Investigation, Validation, Visualization. KS: Data curation, Investigation, Writing – review & editing. BA: Investigation, Data curation, Writing – review & editing. NV: Investigation, Data curation, Writing – review & editing. RH: Data curation, Investigation, Writing – review & editing, Resources, Validation. BB: Conceptualization, Writing – review & editing. MD: Conceptualization, Data curation, Formal analysis, Funding acquisition, Investigation, Methodology, Project administration, Resources, Supervision, Validation, Visualization, Writing – original draft, Writing – review & editing.

Funding

The author(s) declare financial support was received for the research and/or publication of this article. This work was supported by NIH grant AI143965 to MD.

Acknowledgments

We are grateful to members of the Johns Hopkins Division of Allergy and Clinical Immunology for insightful discussions and help, especially Dr. Donald MacGlashan. We also thank the Bayview Immunomics Core (BIC) for assistance with flow cytometry service.

Conflict of interest

Author MD has consulted and/or participated on advisory boards for Aditum Bio, ALK, Allakos, Blueprint Medicines, Guidepoint, GLG, Melinta Therapeutics, Nurix Therapeutics, and Telios Pharma, and has received funding from AstraZeneca.

The remaining authors declare that the research was conducted in the absence of any commercial or financial relationships that could be construed as a potential conflict of interest.

The author(s) declared that they were an editorial board member of Frontiers, at the time of submission. This had no impact on the peer review process and the final decision.

Generative AI statement

The author(s) declare that no Generative AI was used in the creation of this manuscript.

Publisher's note

Supplementary material

The Supplementary Material for this article can be found online at: https://www.frontiersin.org/articles/10.3389/fimmu.2025.1628194/full#supplementary-material

References

1. Prochazka M, Gaskins HR, Shultz LD, Leiter EH. The nonobese diabetic scid mouse: model for spontaneous thymomagenesis associated with immunodeficiency. *Proc Natl Acad Sci*. (1992) 89:3290–4. doi: 10.1073/pnas.89.8.3290

2. Ishikawa F, Yasukawa M, Lyons B, Yoshida S, Miyamoto T, Yoshimoto G, et al. Development of functional human blood and immune systems in NOD/SCID/IL2 receptor γ chainnull mice. *Blood*. (2005) 106:1565–73. doi: 10.1182/blood-2005-02-0516

3. Shultz LD, Lyons BL, Burzenski LM, Gott B, Chen X, Chaleff S, et al. Human Lymphoid and Myeloid Cell Development in NOD/LtSz- *scid IL2R γ null* Mice Engrafted with Mobilized Human Hemopoietic Stem Cells. *J Immunol*. (2005) 174:6477–89. doi: 10.4049/jimmunol.174.10.6477

4. Wunderlich M, Chou FS, Sexton C, Presicce P, Chougnet CA, Aliberti J, et al. Improved multilineage human hematopoietic reconstitution and function in NSGS mice. Stoddart CA, editor. *PloS One*. (2018) 13:e0209034. doi: 10.1371/journal.pone.0209034

5. Bryce PJ, Falahati R, Kenney LL, Leung J, Bebbington C, Tomasevic N, et al. Humanized mouse model of mast cell–mediated passive cutaneous anaphylaxis and passive systemic anaphylaxis. *J Allergy Clin Immunol*. (2016) 138:769–79. doi: 10.1016/j.jaci.2016.01.049

6. Greenblatt MB, Vbranac V, Tivey T, Tsang K, Tager AM, Aliprantis AO. Graft versus Host Disease in the Bone Marrow, Liver and Thymus Humanized Mouse Model. Stoddart CA, editor. *PloS One*. (2012) 7:e44664. doi: 10.1371/journal.pone.0044664

7. Skelton JK, Ortega-Prieto AM, Dorner M. A Hitchhiker's guide to humanized mice: new pathways to studying viral infections. *Immunology*. (2018) 154:50–61. doi: 10.1111/imm.12906

8. Dispenza MC, Krier-Burris RA, Chhiba KD, Undem BJ, Robida PA, Bochner BS. Bruton's tyrosine kinase inhibition effectively protects against human IgE-mediated anaphylaxis. *J Clin Invest*. (2020) 130:4759–70. doi: 10.1172/JCI138448

9. Nicolini FE, Cashman JD, Hogge DE, Humphries RK, Eaves CJ. NOD/SCID mice engineered to express human IL-3, GM-CSF and Steel factor constitutively mobilize engrafted human progenitors and compromise human stem cell regeneration. *Leukemia*. (2004) 18:341–7. doi: 10.1038/sj.leu.2403222

10. Billerbeck E, Barry WT, Mu K, Dorner M, Rice CM, Ploss A. Development of human CD4+FoxP3+ regulatory T cells in human stem cell factor–, granulocyte-macrophage colony-stimulating factor–, and interleukin-3–expressing NOD-SCID IL2Rγnull humanized mice. *Blood*. (2011) 117:3076–86. doi: 10.1182/blood-2010-08-301507

11. Burton OT, Stranks AJ, Tamayo JM, Koleoglou KJ, Schwartz LB, Oettgen HC. A humanized mouse model of anaphylactic peanut allergy. *J Allergy Clin Immunol*. (2017) 139:314–22. doi: 10.1016/j.jaci.2016.04.034

12. Alakhras NS, Shin J, Smith SA, Sinn AL, Zhang W, Hwang G, et al. Peanut allergen inhibition prevents anaphylaxis in a humanized mouse model. *Sci Transl Med*. (2023) 15:eadd6373. doi: 10.1126/scitranslmed.add6373

13. Youngblood BA, Brock EC, Leung J, Falahati R, Bryce PJ, Bright J, et al. AK002, a humanized sialic acid-binding immunoglobulin-like lectin-8 antibody that induces antibody-dependent cell-mediated cytotoxicity against human eosinophils and inhibits mast cell-mediated anaphylaxis in mice. *Int Arch Allergy Immunol*. (2019) 180:91–102. doi: 10.1159/000501637

14. O'Brien LJ, Walpole CM, Leal-Rojas IM, Shatunova S, Moore A, Winkler IG, et al. Characterization of human engraftment and hemophagocytic lymphohistiocytosis in NSG-SGM3 neonate mice engrafted with purified CD34+ Hematopoietic stem cells. *Exp Hematol*. (2024) 130:104134. doi: 10.1016/j.exphem.2023.11.008

15. Wunderlich M, Stockman C, Devarajan M, Ravishankar N, Sexton C, Kumar AR, et al. A xenograft model of macrophage activation syndrome amenable to anti-CD33 and anti–IL-6R treatment. *JCI Insight*. (2016) 1(15):e88181. Available online at: https://insight.jci.org/articles/view/88181.

16. Janke LJ, Imai DM, Tillman H, Doty R, Hoenerhoff MJ, Xu JJ, et al. Development of mast cell and eosinophil hyperplasia and HLH/MAS-like disease in NSG-SGM3 mice receiving human CD34+ Hematopoietic stem cells or patient-derived leukemia xenografts. *Vet Pathol*. (2021) 58:181–204. doi: 10.1177/0300985820970144

17. Hung S, Kasperkowitz A, Kurz F, Dreher L, Diessner J, Ibrahim ES, et al. Next-generation humanized NSG-SGM3 mice are highly susceptible to Staphylococcus aureus infection. *Front Immunol*. (2023) 14:1127709. doi: 10.3389/fimmu.2023.1127709

18. Jangalwe S, Shultz LD, Mathew A, Brehm MA. Improved B cell development in humanized NOD-scid IL2Rγ mice transgenically expressing human stem cell factor, granulocyte-macrophage colony-stimulating factor and interleukin-3. *Immun Inflammation Dis*. (2016) 4:427–40. doi: 10.1002/iid3.124

19. Hamilton RG, Croote D, Lupinek C, Matsson P. Evolution toward chip-based arrays in the laboratory diagnosis of human allergic disease. *J Allergy Clin Immunol Pract*. (2023) 11:2991–9. doi: 10.1016/j.jaip.2023.08.017

20. Hamilton RG, Holbreich M, Bronzert C, Anderson RL, Schoettler N, Ober C. Screening asthmatics for atopic status using the ALergy EXplorer (ALEX2) macroarray. *J Asthma*. (2024) 61:1050–7. doi: 10.1080/02770903.2024.2324839

21. Altmann F. Coping with cross-reactive carbohydrate determinants in allergy diagnosis. *Allergo J Int*. (2016) 25:98–105. doi: 10.1007/s40629-016-0115-3

22. Vaidyanathan B, Chaudhry A, Yewdell WT, Angeletti D, Yen WF, Wheatley AK, et al. The aryl hydrocarbon receptor controls cell-fate decisions in B cells. *J Exp Med*. (2017) 214:197–208. doi: 10.1084/jem.20160789

23. Lim J, Lin EV, Hong JY, Vaidyanathan B, Erickson SA, Annicelli C, et al. Induction of natural IgE by glucocorticoids. *J Exp Med*. (2022) 219:e20220903. doi: 10.1084/jem.20220903

24. Dispenza MC, Metcalfe DD, Olivera A. Research advances in mast cell biology and their translation into novel therapies for anaphylaxis. *J Allergy Clin Immunol Pract*. (2023) 11:2032–42. doi: 10.1016/j.jaip.2023.03.015

25. Wong CY, Yeh KW, Huang JL, Su KW, Tsai MH, Hua MC, et al. Longitudinal analysis of total serum IgE levels with allergen sensitization and atopic diseases in early childhood. *Sci Rep*. (2020) 10:21278. doi: 10.1038/s41598-020-78272-8

26. Qiu C, Zhong L, Huang C, Long J, Ye X, Wu J, et al. Cell-bound IgE and plasma IgE as a combined clinical diagnostic indicator for allergic patients. *Sci Rep*. (2020) 10:4700. doi: 10.1038/s41598-020-61455-8

27. Gonzalez-Quintela A, Alende R, Gude F, Campos J, Rey J, Meijide LM, et al. Serum levels of immunoglobulins (IgG, IgA, IgM) in a general adult population and their relationship with alcohol consumption, smoking and common metabolic abnormalities. *Clin Exp Immunol*. (2008) 151:42–50. doi: 10.1111/j.1365-2249.2007.03545.x

28. Dati F, Schumann G, Thomas L, Aguzzi F, Baudner S, Bienvenu J, et al. Consensus of a group of professional societies and diagnostic companies on guidelines for interim reference ranges for 14 proteins in serum based on the standardization against the IFCC/BCR/CAP Reference Material (CRM 470). International Federation of Clinical Chemistry. Community Bureau of Reference of the Commission of the European Communities. College of American Pathologists. *Eur J Clin Chem Clin Biochem J Forum Eur Clin Chem Soc*. (1996) 34:517–20.

29. Patel P, Jamal Z, Ramphul K. Immunoglobulin. In: *StatPearls*. StatPearls Publishing, Treasure Island (FL (2025). Available online at: http://www.ncbi.nlm.nih.gov/books/NBK513460/.

30. Coughlan AM, Harmon C, Whelan S, O'Brien EC, O'Reilly VP, Crotty P, et al. Myeloid engraftment in humanized mice: impact of granulocyte-colony stimulating factor treatment and transgenic mouse strain. *Stem Cells Dev*. (2016) 25:530–41. doi: 10.1089/scd.2015.0289

31. Arican O, Aral M, Sasmaz S, Ciragil P. Serum levels of TNF-α, IFN-γ, IL-6, IL-8, IL-12, IL-17, and IL-18 in patients with active psoriasis and correlation with disease severity. *Mediators Inflamm*. (2005) 2005:273–9. doi: 10.1155/MI.2005.273

32. Martin K, Viera K, Petr C, Marie N, Eva T. Simultaneous analysis of cytokines and costimulatory molecules concentrations by ELISA technique and of probabilities of measurable concentrations of interleukins IL-2, IL-4, IL-5, IL-6, CXCL8 (IL-8), IL-10, IL-13 occurring in plasma of healthy blood donors. *Mediators Inflamm*. (2006) 2006:65237. doi: 10.1155/MI/2006/65237

33. Lee YJ, Holzapfel KL, Zhu J, Jameson SC, Hogquist KA. Steady-state production of IL-4 modulates immunity in mouse strains and is determined by lineage diversity of iNKT cells. *Nat Immunol*. (2013) 14:1146–54. doi: 10.1038/ni.2731

34. Popko K, Gorska E, Stelmaszczyk-Emmel A, Plywaczewski R, Stoklosa A, Gorecka D, et al. Proinflammatory cytokines Il-6 and TNF-α and the development of inflammation in obese subjects. *Eur J Med Res*. (2010) 15 Suppl 2:120–2. doi: 10.1186/2047-783x-15-s2-120

35. Dent AL, Doherty TM, Paul WE, Sher A, Staudt LM. BCL-6-deficient mice reveal an IL-4-independent, STAT6-dependent pathway that controls susceptibility to infection by leishmania major. *J Immunol*. (1999) 163:2098–103. doi: 10.4049/jimmunol.163.4.2098

36. Weskamm LM, Dahlke C, Addo MM. Flow cytometric protocol to characterize human memory B cells directed against SARS-CoV-2 spike protein antigens. *STAR Protoc*. (2022) 3:101902. doi: 10.1016/j.xpro.2022.101902

37. Weisel NM, Joachim SM, Smita S, Callahan D, Elsner RA, Conter LJ, et al. Surface phenotypes of naive and memory B cells in mouse and human tissues. *Nat Immunol*. (2022) 23:135–45. doi: 10.1038/s41590-021-01078-x

38. Weisel F, Shlomchik M. Memory B cells of mice and humans. *Annu Rev Immunol*. (2017) 35:255–84. doi: 10.1146/annurev-immunol-041015-055531

39. Koenig JFE, Knudsen NPH, Phelps A, Bruton K, Hoof I, Lund G, et al. Type 2–polarized memory B cells hold allergen-specific IgE memory. *Sci Transl Med*. (2024) 16: eadi0944. doi: 10.1126/scitranslmed.adi0944

40. Kraft S, Kinet JP. New developments in FcεRI regulation, function and inhibition. *Nat Rev Immunol*. (2007) 7:365–78. doi: 10.1038/nri2072

41. Lanzavecchia A, Sallusto F. Human B cell memory. *Curr Opin Immunol*. (2009) 21:298–304. doi: 10.1016/j.coi.2009.05.019

42. Hong SW OE, Lee JY, Lee M, Han D, Ko HJ, Sprent J, et al. Food antigens drive spontaneous IgE elevation in the absence of commensal microbiota. *Sci Adv*. (2019) 5: eaaw1507. doi: 10.1126/sciadv.aaw1507

43. Fernandes-Braga W, Curotto de Lafaille MA. B cell memory of Immunoglobulin E (IgE) antibody responses in allergy. *Curr Opin Immunol*. (2024) 91:102488. doi: 10.1016/j.coi.2024.102488

44. He JS, Subramaniam S, Narang V, Srinivasan K, Saunders SP, Carbajo D, et al. IgG1 memory B cells keep the memory of IgE responses. *Nat Commun*. (2017) 8:641. doi: 10.1038/s41467-017-00723-0

45. Hoof I, Schulten V, Layhadi JA, Stranzl T, Christensen LH, de la MSH, et al. Allergen-specific IgG+ memory B cells are temporally linked to IgE memory responses. *J Allergy Clin Immunol*. (2020) 146:180–91. doi: 10.1016/j.jaci.2019.11.046

46. Laffleur B, Debeaupuis O, Dalloul Z, Cogné M. B cell intrinsic mechanisms constraining igE memory. *Front Immunol*. (2017) 8. doi: 10.3389/fimmu.2017.01277

47. Laffleur B, Duchez S, Tarte K, Denis-Lagache N, Péron S, Carrion C, et al. Self-restrained B cells arise following membrane igE expression. *Cell Rep*. (2015) 10:900–9. doi: 10.1016/j.celrep.2015.01.023

48. Haniuda K, Fukao S, Kitamura D. Metabolic reprogramming induces germinal center B cell differentiation through bcl6 locus remodeling. *Cell Rep*. (2020) 33:108333. doi: 10.1016/j.celrep.2020.108333

49. Yang Z, Sullivan BM, Allen CDC. Fluorescent *in vivo* detection reveals that igE+ B cells are restrained by an intrinsic cell fate predisposition. *Immunity*. (2012) 36:857–72. doi: 10.1016/j.immuni.2012.02.009

50. Yang Z, Robinson MJ, Chen X, Smith GA, Taunton J, Liu W, et al. Regulation of B cell fate by chronic activity of the IgE B cell receptor. *eLife*. (2016) 5:e21238. doi: 10.7554/eLife.21238

51. Talay O, Yan D, Brightbill HD, Straney EEM, Zhou M, Ladi E, et al. IgE+ memory B cells and plasma cells generated through a germinal-center pathway. *Nat Immunol*. (2012) 13:396–404. doi: 10.1038/ni.2256

52. Talay O, Yan D, Brightbill H, Straney E, Zhou M, Ladi E, et al. Direct detection of IgE-switched B cells in an IgE-GFP reporter mouse reveals a germinal center pathway for the generation of IgE memory B cells and plasma cells (109.3). *J Immunol*. (2012) 188:109.3–3. doi: 10.4049/jimmunol.188.Supp.109.3

53. Lin W, Truong N, Grossman WJ, Haribhai D, Williams CB, Wang J, et al. Allergic dysregulation and hyperimmunoglobulinemia E in Foxp3 mutant mice. *J Allergy Clin Immunol*. (2005) 116:1106–15. doi: 10.1016/j.jaci.2005.08.046

54. Cahenzli J, Köller Y, Wyss M, Geuking MB, McCoy KD. Intestinal microbial diversity during early-life colonization shapes long-term IgE levels. *Cell Host Microbe*. (2013) 14:559–70. doi: 10.1016/j.chom.2013.10.004

55. Grunewald SM, Kunzmann S, Schnarr B, Ezernieks J, Sebald W, Duschl A. A murine interleukin-4 antagonistic mutant protein completely inhibits interleukin-4-induced cell proliferation, differentiation, and signal transduction. *J Biol Chem*. (1997) 272:1480–3. doi: 10.1074/jbc.272.3.1480

56. Andrews RP, Rosa LR, Daines MO, Khurana Hershey GK. Reconstitution of a functional human type II IL-4/IL-13 receptor in mouse B cells: demonstration of species specificity1. *J Immunol*. (2001) 166:1716–22. doi: 10.4049/jimmunol.166.3.1716

57. Sinclair D, Peters SA. The predictive value of total serum IgE for a positive allergen specific IgE result. *J Clin Pathol*. (2004) 57:956–9. doi: 10.1136/jcp.2004.017681

58. Sampson HA, O'Mahony L, Burks AW, Plaut M, Lack G, Akdis CA. Mechanisms of food allergy. *J Allergy Clin Immunol*. (2018) 141:11–9. doi: 10.1016/j.jaci.2017.11.005

59. Sicherer SH, Sampson HA. Food allergy: A review and update on epidemiology, pathogenesis, diagnosis, prevention, and management. *J Allergy Clin Immunol*. (2018) 141:41–58. doi: 10.1016/j.jaci.2017.11.003

60. Meng Y, Nerlov C. Epigenetic regulation of hematopoietic stem cell fate. *Trends Cell Biol*. (2025) 35:217–29. doi: 10.1016/j.tcb.2024.08.005

61. Allakhverdi Z, Comeau MR, Smith DE, Toy D, Endam LM, Desrosiers M, et al. CD34+ hemopoietic progenitor cells are potent effectors of allergic inflammation. *J Allergy Clin Immunol*. (2009) 123:472–8. doi: 10.1016/j.jaci.2008.10.022

62. Mohanan MM, Shetty R, Bang-Berthelsen CH, Mudnakudu-Nagaraju KK. Role of mesenchymal stem cells and short chain fatty acids in allergy: A prophylactic therapy for future. *Immunol Lett*. (2023) 260:1–10. doi: 10.1016/j.imlet.2023.06.002

63. Almgren M, Schlinzig T, Gomez-Cabrero D, Gunnar A, Sundin M, Johansson S, et al. Cesarean delivery and hematopoietic stem cell epigenetics in the newborn infant: implications for future health? *Am J Obstet Gynecol*. (2014) 211:502.e1–8. doi: 10.1016/j.ajog.2014.05.014

64. Wesemann DR, Portuguese AJ, Meyers RM, Gallagher MP, Cluff-Jones K, Magee JM, et al. Microbial colonization influences early B-lineage development in the gut lamina propria. *Nature*. (2013) 501:112–5. doi: 10.1038/nature12496

65. Shade KTC, Platzer B, Washburn N, Mani V, Bartsch YC, Conroy M, et al. A single glycan on IgE is indispensable for initiation of anaphylaxis. *J Exp Med*. (2015) 212:457–67. doi: 10.1084/jem.20142182

66. Shade KTC, Conroy ME, Washburn N, Kitaoka M, Huynh DJ, Laprise E, et al. Sialylation of immunoglobulin E is a determinant of allergic pathogenicity. *Nature*. (2020) 582:265–70. doi: 10.1038/s41586-020-2311-z

67. Shade KTC, Anthony RM. Antibody glycosylation and inflammation. *Antibodies*. (2013) 2:392–414. doi: 10.3390/antib2030392

68. Engeroff P, Caviezel F, Mueller D, Thoms F, Bachmann MF, Vogel M. CD23 provides a noninflammatory pathway for IgE-allergen complexes. *J Allergy Clin Immunol*. (2020) 145:301–11. doi: 10.1016/j.jaci.2019.07.045

69. Selb R, Eckl-Dorna J, Neunkirchner A, Schmetterer K, Marth K, Gamper J, et al. CD23 surface density on B cells is associated with IgE levels and determines IgE-facilitated allergen uptake, as well as activation of allergen-specific T cells. *J Allergy Clin Immunol*. (2017) 139:290–9. doi: 10.1016/j.jaci.2016.03.042

70. Kisselgof AB, Oettgen HC. The expression of murine B cell CD23, *in vivo*, is regulated by its ligand, IgE. *Int Immunol*. (1998) 10:1377–84. doi: 10.1093/intimm/10.9.1377

71. Xiong H, Dolpady J, Wabl M, Curotto de Lafaille MA, Lafaille JJ. Sequential class switching is required for the generation of high affinity IgE antibodies. *J Exp Med*. (2012) 209:353–64. doi: 10.1084/jem.20111941

72. Wu YL, Stubbington MJT, Daly M, Teichmann SA, Rada C. Intrinsic transcriptional heterogeneity in B cells controls early class switching to IgE. *J Exp Med*. (2017) 214:183–96. doi: 10.1084/jem.20161056

73. Wesemann DR, Magee JM, Boboila C, Calado DP, Gallagher MP, Portuguese AJ, et al. Immature B cells preferentially switch to IgE with increased direct Sμ to Sε recombination. *J Exp Med*. (2011) 208:2733–46. doi: 10.1084/jem.20111155

74. McCoy KD, Harris NL, Diener P, Hatak S, Odermatt B, Hangartner L, et al. Natural igE production in the absence of MHC class II cognate help. *Immunity*. (2006) 24:329–39. doi: 10.1016/j.immuni.2006.01.013

75. Crawford G, Hayes MD, Seoane RC, Ward S, Dalessandri T, Lai C, et al. Epithelial damage and tissue γδ T cells promote a unique tumor-protective IgE response. *Nat Immunol*. (2018) 19:859–70. doi: 10.1038/s41590-018-0161-8

76. Hayes MD, Ward S, Crawford G, Seoane RC, Jackson WD, Kipling D, et al. Inflammation-induced IgE promotes epithelial hyperplasia and tumour growth. Harris NL, Rath S, Harris NL, Robinson M, editors. *eLife*. (2020) 9:e51862. doi: 10.7554/eLife.51862